Proceedings of the 4th International Conference on Environmental Geoscience and Earth Ecology
DOI: 10.54254/2753-8818/2026.34289

Analysis of Tree Microstructure via Laser Diffraction for Climate Change Tracking

Xinxiang Pu

Shanghai Starriver Bilingual School, Shanghai, China
gamila.wu@qq.com

Abstract. Climate change is a critical global issue. Traditional climate research often depends on costly equipment and complex systems, making it less accessible to the public. This study uses laser diffraction to quantitatively analyze historical tree growth and machine learning to explore links between climate change and tree development. Results show that tree microstructural size is positively correlated with annual precipitation and sunlight, with sunlight having a stronger effect. Lower annual average high and low temperatures were associated with faster growth, while higher average temperatures led to lush growth. Predictions for future tree growth and climate trends, based on historical data, have been partially verified. This study offers a practical method for analyzing tree microstructures and demonstrates that tree-based climate analysis is both accurate and applicable.

Keywords: laser diffraction, tree microscopy, machine learning, climate change

1. Introduction

1.1. Background

Global temperatures have risen by about 1.2°C relative to pre-industrial levels [1], contributing to more frequent extreme climate events. Conventional monitoring using satellites and weather stations mainly captures short-term conditions and incurs high costs. Tree rings offer a biological record, reflecting annual growth variations sensitive to environmental changes. This study uses a custom laser diffractometer to analyze cellulose microstructure in tree xylem and examines the relationship between ring characteristics and historical climate records, providing an accessible approach for reconstructing past climate variability.

1.2. Related work

X-ray diffraction (XRD) is widely used to study wood cellulose due to its non-destructive nature, allowing quantification of parameters like helical angles and crystallinity [2-4]. Chemical treatments, such as NaOH, can alter cellulose I to II depending on concentration and duration. Microscopic methods complement diffraction studies: laser scanning confocal microscopy enables rapid cross-sectional analysis of pulp fibers [5], and combined microprobes reveal both microstructure and chemical composition in petrified wood [6]. Environmental factors strongly

© 2026 The Authors. This is an open access article distributed under the terms of the Creative Commons Attribution License 4.0 (https://creativecommons.org/licenses/by/4.0/).

DOI: 10.54254/2753-8818/2026.34289

affect xylem structure, with temperature influencing cambial activity and lignification [7], making tree rings valuable climate archives [8-10]. Although dendroclimatology often relies on macroscopic indicators, integrating microstructural analysis could enhance paleoclimate reconstructions.

1.3. Research content

This study presents a portable laser diffraction system (632 nm) to investigate the relationship between cellulose microstructure and climate variability (Figure 1).

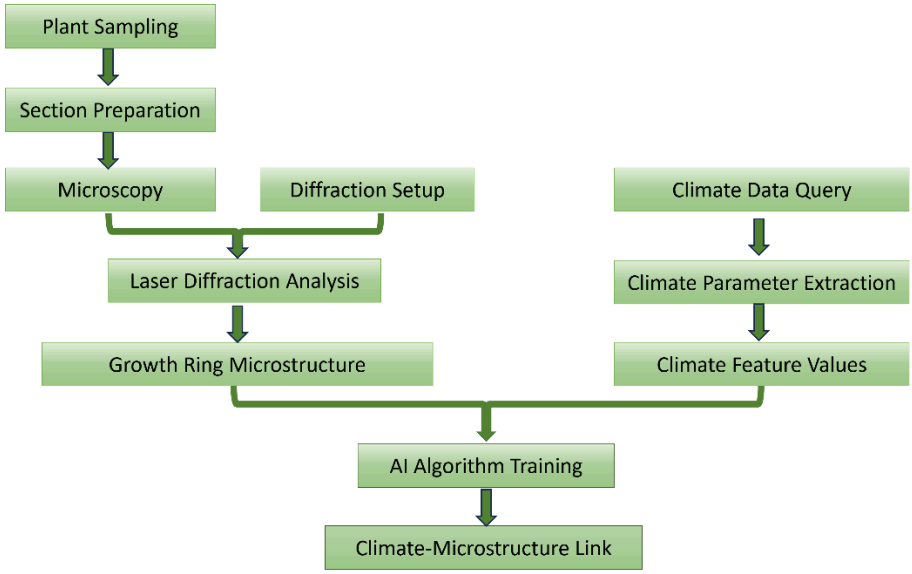

Figure 1. Technical approach

Thin xylem sections (<100 μm) are prepared for optical measurement, and CCD-based diffraction captures cellulose lattice variations. These microstructural features are analyzed alongside historical climate records using machine learning. Compared with traditional methods, this approach emphasizes microstructure, offers a non-destructive alternative to X-ray or mechanical testing, and relies on relatively simple instrumentation.

2. Theoretical foundation

2.1. Interference and diffraction of light

Light exhibits wave-particle duality, with its wave nature explaining phenomena such as colorful soap bubble interference patterns and 3D cinema effects. Light propagates as a transverse electromagnetic wave, with perpendicular electric and magnetic fields. Phase differences create wave surfaces and wavefronts, the latter representing the leading edge of the wave. Light intensity corresponds to the average energy flux, primarily determined by the electric field (Figure 2).

DOI: 10.54254/2753-8818/2026.34289

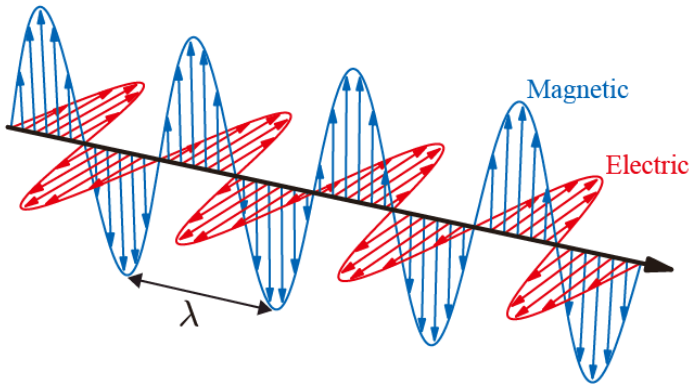

Figure 2. Schematic diagram of light as a transverse electromagnetic wave

Light interference requires stable phase, matched frequency, and polarization. Ordinary light from spontaneous emission typically lacks coherence. By contrast, laser radiation, generated via stimulated emission in an optical resonator, is highly coherent, monochromatic, and directional, making it ideal for interference measurements. Classical experiments, like Young's double-slit, often require spatial filtering when using conventional light sources to produce clear patterns.

Grating diffraction, based on multi-slit interference (with slit spacing d), follows $d\sin\theta = m\lambda$, where angular dispersion $\Delta\theta/\Delta\lambda = m/(d\cos\theta)$ governs resolution. Plant xylem's lignin microstructure acts as a natural 2D grating; laser diffraction fringe analysis leverages these principles to measure micrometer-scale structural details.

2.2. Analysis of microstructure components of trees

Wood microstructures influence optical diffraction at the micron scale. Vessels (10-300 μm) produce grating-like or diffuse ring patterns depending on arrangement. Fibers (10-30 μm diameter, up to 1.5 mm length) generate directional features, while conifer tracheids (10-85 μm) contribute strong signals and ray cells (10-50 μm) induce anisotropic patterns. Differences between primary and secondary cell wall layers further affect diffraction. Regular structures can be modeled as gratings, whereas irregular regions, such as bark, are better described using scattering or Fraunhofer approximations.

3. Simulation calculations of laser diffraction

When the screen is sufficiently far from the grating, diffraction patterns approximate planar wave superposition (Fraunhofer regime). The intensity distribution on the image plane can be calculated as:

$$U(x,y) = \frac{e^{ikz}e^{i\frac{k}{2z}(x^2+y^2)}}{i\lambda z}\iint_{-\infty}^{\infty} u(x',y')e^{-i\frac{2\pi}{\lambda z}(x'x+y'y)}dx'dy' \quad (1)$$

Longitudinal wood sections display fibrous, grid-like patterns that can be modeled as one-dimensional gratings. MATLAB simulations with a 632.8 nm laser show that diffraction spot spacing decreases as the grating constant increases, and increases with screen distance (0.5-4 m), ranging from 1.8 cm to 15 cm. Intensity gradually diminishes from the central maximum to peripheral spots, consistent with classical diffraction theory, indicating the applicability of grating models to wood microstructures.

DOI: 10.54254/2753-8818/2026.34289

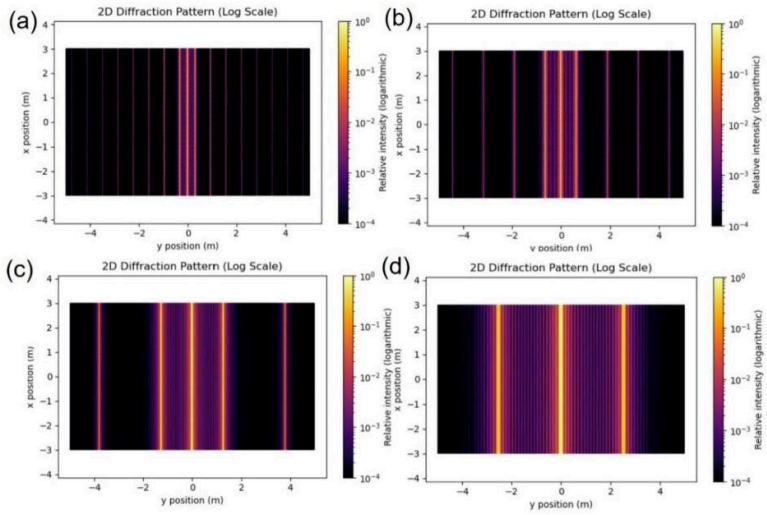

Figure 3. Simulated diffraction patterns with varied grating constants: (a) 0.5μm, (b) 1μm, (c) 2μm, (d) 4μm

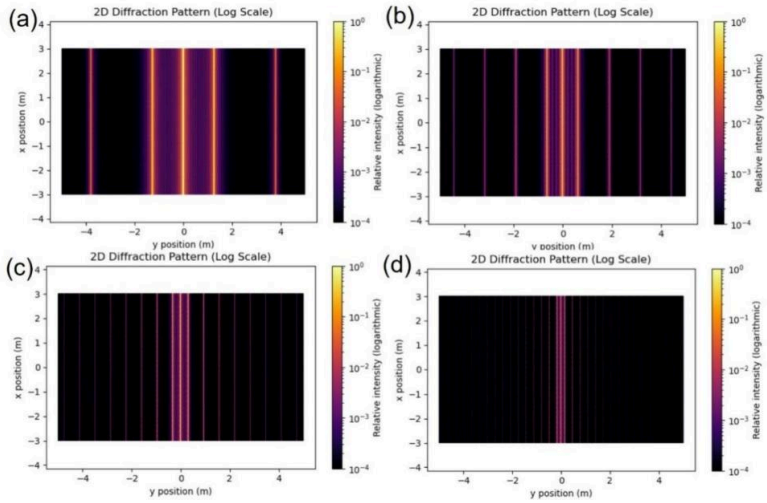

Figure 4. Simulated diffraction patterns with varied grating constants: (a) 0.5m, (b) 1m, (c) 2m, (d) 4m

4. Experimental procedure

(1) **Sample Preparation**: Ø5cm×15cm wood samples were boiled (24hrs), sectioned longitudinally to <100μm slices (>0.1cm²), meeting laser diffraction requirements (632nm, 50mW, 15mm spot at 40cm).

(2) **Instrument Setup**: A 632.8nm laser system (Figure.5) with CCD detector recorded real-time diffraction patterns from samples positioned at the focal spot.

(3) **Microstructure Analysis**: Diffraction spots were analyzed by $\overline{d_I} = \frac{D\lambda}{\overline{x_{I/2}}}$, where D is sample-to-screen distance, λ is laser wavelength (632.8 nm), and $\overline{x_1}$ is average diffraction spot spacing.

(4) **Climate Correlation**: Microstructural dimensions were cross-referenced with historical temperature/precipitation data to quantify climate-growth relationships.

DOI: 10.54254/2753-8818/2026.34289

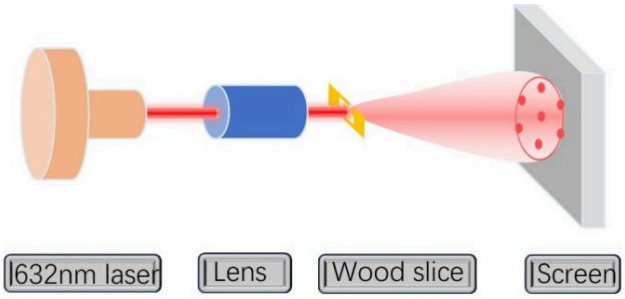

Figure 5. Schematic diagram of laser diffraction optical path

5. Experimental results

5.1. Grating diffraction experiment

Initial verification used 1D gratings (d=0.05-0.2mm) in the setup shown in Figure.6a. Diffraction patterns (Figure.6b) exhibited alternating bright/dark spots with spacing responsive to changes in *d* or distance *D*. Experimental data for different gratings (Figures.6c-d) confirmed theoretical predictions, validating the methodology.

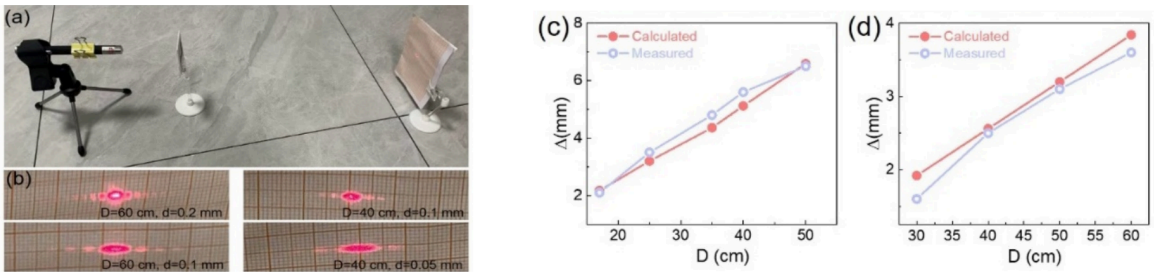

Figure 6. Grating diffraction experiment (a) Setup schematic, (b) Laser diffraction pattern, (c)-(d) Spot spacing vs. distance D for d=0.1mm and 0.2mm gratings

5.2. Tree slice diffraction experiment

A 3.5 cm diameter osmanthus branch sample (1.7 m above ground) was sectioned into 0.5-1 cm long, 0.2 mm thick slices with moderate transparency (Figure. 7a). Microscopic analysis revealed disordered fibrous structures at low magnification, while higher magnification clearly showed regular periodic grid patterns with approximately 20 μm spacing.

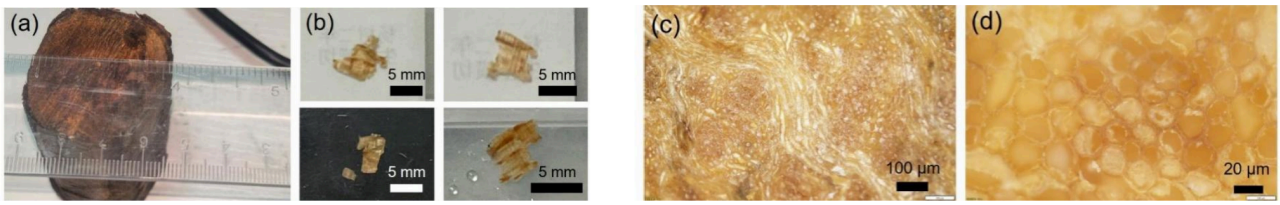

Figure 7. Osmanthus wood processing. (a) Raw sample, (b) Cross-section, (c) Low-mag view, (d) Microstructure (high-mag)

DOI: 10.54254/2753-8818/2026.34289

Diffraction analysis revealed faint, discontinuous spots, indicating short-range (but not long-range) periodicity in fiber structure, consistent with Figure.7 microscopy. Measured 9.8-9.9 mm spot spacing (Figure.8) corresponded to about 28 μm microstructure spacing, matching microscopic observations.

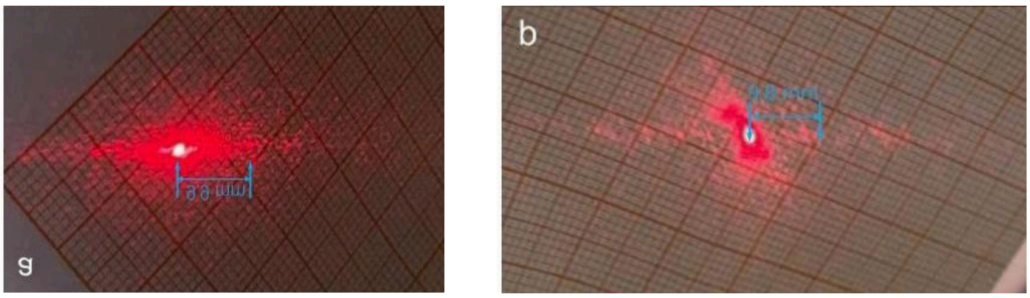

Figure 8. Laser Diffraction of Osmanthus Sections: (a) Surface region diffraction pattern; (b) Deep layer diffraction pattern

The inherent hardness and dark pigmentation of osmanthus wood posed significant sectioning challenges, yielding samples with inadequate transparency that either completely blocked laser transmission or produced edge-gap diffraction artifacts. To enhance signal detection, proposed improvements include: increasing laser power output, selecting softer wood species to improve section quality and light transmittance (preliminarily verifiable by backlight inspection), and extending the sample-to-screen distance to amplify diffraction spacing from millimeter to centimeter scale for improved measurement precision.

Fir wood samples (7.8 cm diameter, 14 growth rings) collected from Zhangjiajie, Hunan in 2024 were processed by boiling in water at 100°C for 12 hours to remove resin, then sectioned longitudinally. Microscopic examination revealed a more regular structure compared to osmanthus wood, displaying uniformly distributed elongated features with widths of 20-200 μm (Figure.9). Using a 50mW adjustable-focus laser in a darkroom environment with precise focusing, clear periodic diffraction patterns were successfully obtained (Figure.10). Fiber diameter was calculated by measuring diffraction spacing and sample-to-screen distance. Quantitative growth data across different annual rings were extracted (Table 1), enabling historical growth analysis.

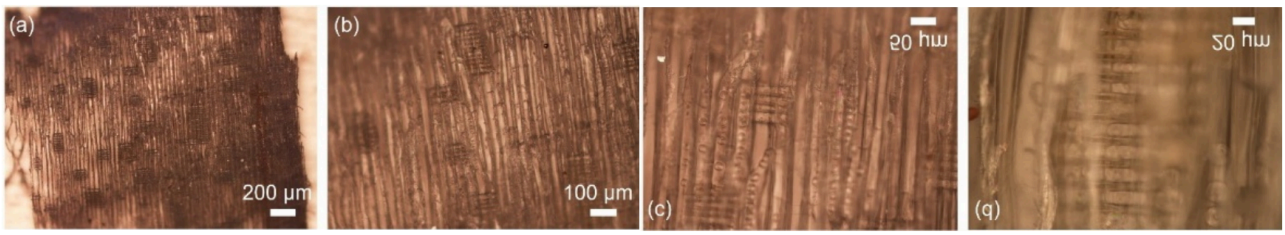

Figure 9. Fir Wood Section Characterization: (a) 5×, (b) 10×, (c) 20×, (d) 50× microscopic images

DOI: 10.54254/2753-8818/2026.34289

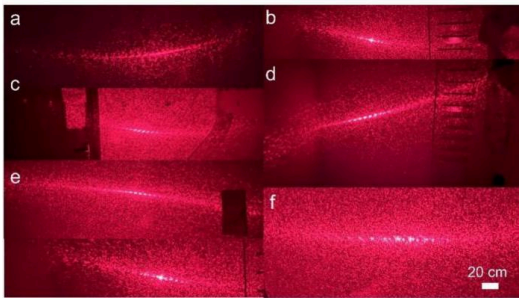

Figure 10. Laser diffraction characterization of fir wood sections

Table 1. Fir section diffraction results & equivalent fiber grid dimensions

Growth Rings	years	x/2(cm)	D(cm)	λ(nm)	d(μm)
-7	2018	5.0	215	632.8	27.2
-6	2019	6.3	215	632.8	21.6
-3	2022	6.0	215	632.8	22.5
-5	2021	4.8	215	632.8	28.3
-5	2020	5.9	215	632.8	23.1
-2	2023	5.5	215	632.8	24.7
-5	2020	4.85	201	632.8	26.2
-3	2022	5	201	632.8	25.4
-9	2016	1	45	632.8	28.5
-8	2017	6.1	215	632.8	22.5

5.3. Analysis of artificial intelligence algorithms

Using meteorological data from Zhangjiajie (Hunan Statistical Yearbook, Table 2), we selected growth-relevant parameters - including mean annual temperature, extreme monthly temperatures (July max/January min), precipitation and sunshine duration - to establish quantitative tree-climate relationships through AI regression modeling.

Table 2. Historical Meteorological Parameters of Zhangjiajie City, Hunan Province

Year	Avg high temp (℃)	Avg low temp (℃)	Mean temp (℃)	Annual precip (mm)	Sunshine hrs/yr
2016	28.7	5.8	18.1	1526.8	1386
2017	30.5	8	18.1	1212	1422
2018	29	4.4	17.9	1240.7	1413
2019	29.2	5.6	17.9	1031	1300
2020	28.5	5.7	16.9	1973	993
2021	28.5	6.4	17.8	1415.2	1337
2021	28.5	6.4	17.8	1415.2	1337
2022	30.9	5.4	18	1056.8	1574
2022	30.9	5.4	18	1056.8	1574
2023	28.3	6.7	17.9	1018.6	1439

DOI: 10.54254/2753-8818/2026.34289

Training with normal equation and gradient descent converged after 250 iterations (Figure.11). Test results (Figure.12) show gradient descent achieved higher accuracy, better matching the 3 samples' actual values. Figure.13 shows: higher temperature inhibits tree growth (extreme heat limits growth); precipitation positively correlates with microstructure size (moisture promotes cell division and metabolism); longer sunlight significantly increases microstructure size (enhanced photosynthesis boosts growth efficiency). All predictions align with scientific principles.

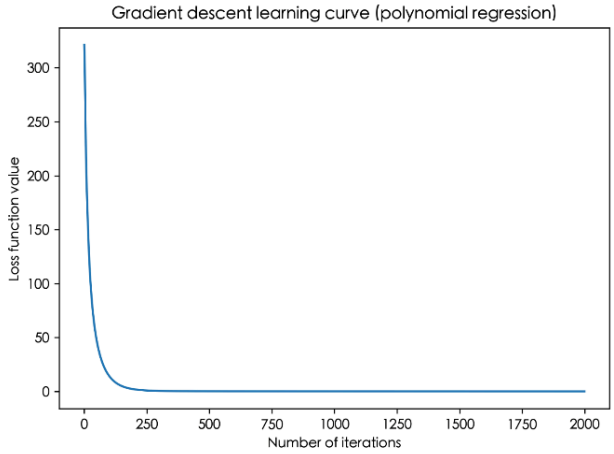

Figure 11. Two-stage regression loss function convergence curve

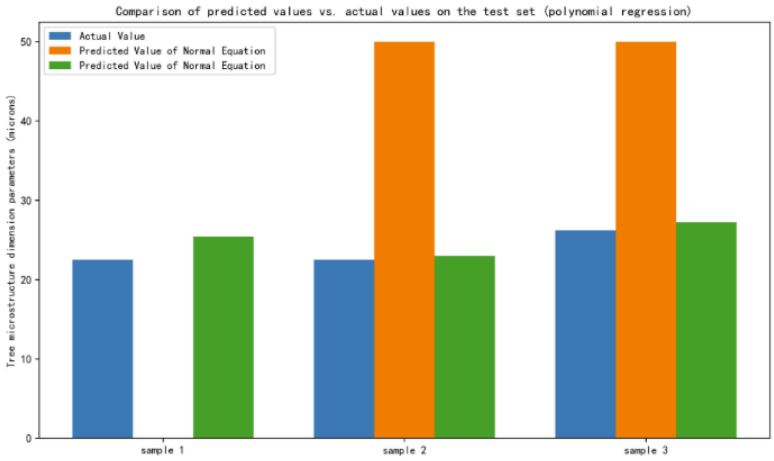

Figure 12. Predicted vs. actual: Two-stage regression (test set)

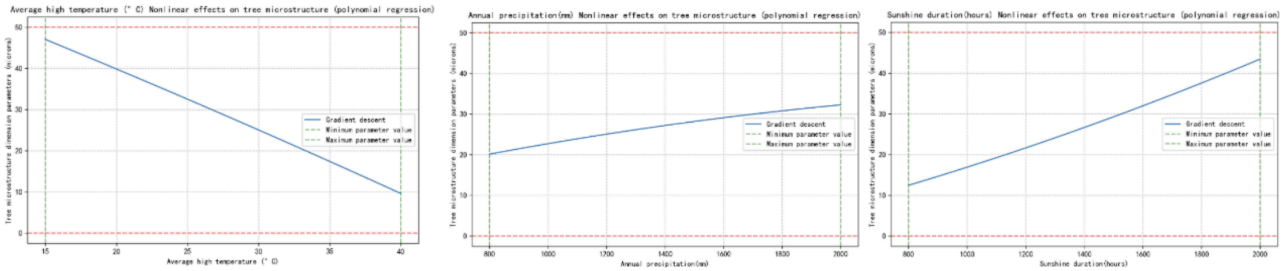

Figure 13. Climate-wood microstructure regression model

DOI: 10.54254/2753-8818/2026.34289

5.4. Prediction of future tree growth conditions and climate conditions

Tree-ring analysis enables prediction of future growth and climate trends. Forecasts based on pre-2023 data (Figure. 14) show that tree microstructure size will decrease year by year from 2024 onward. Combined with the established tree-climate correlation model (Figure. 15), the analysis further predicts a continuing rise in average temperatures for Zhangjiajie, Hunan (Figure. 16).

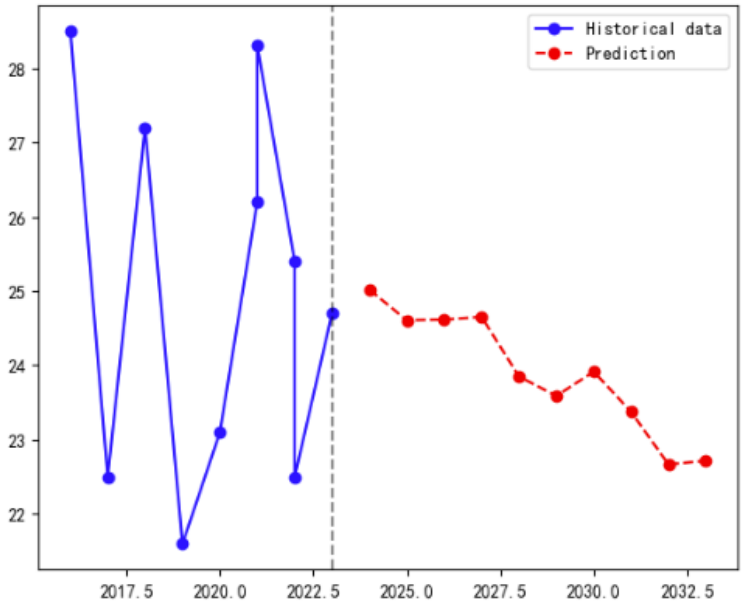

Figure 14. Projecting Chinese fir microstructure evolution (2024-2034)

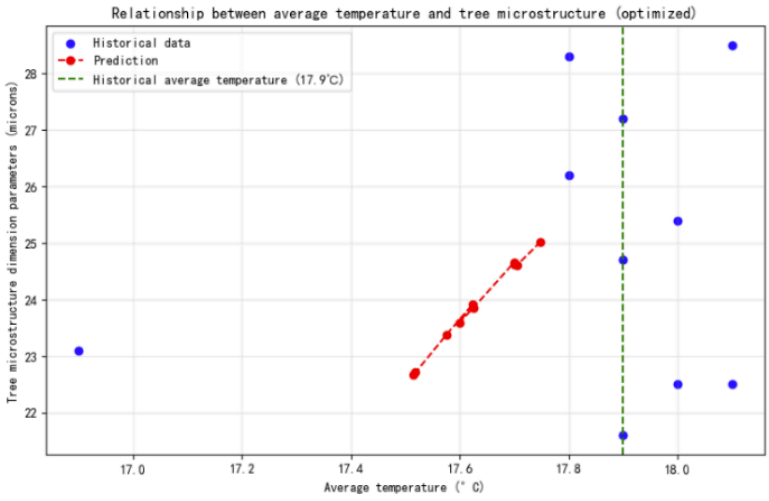

Figure 15. Fir microstructure-temperature correlation

DOI: 10.54254/2753-8818/2026.34289

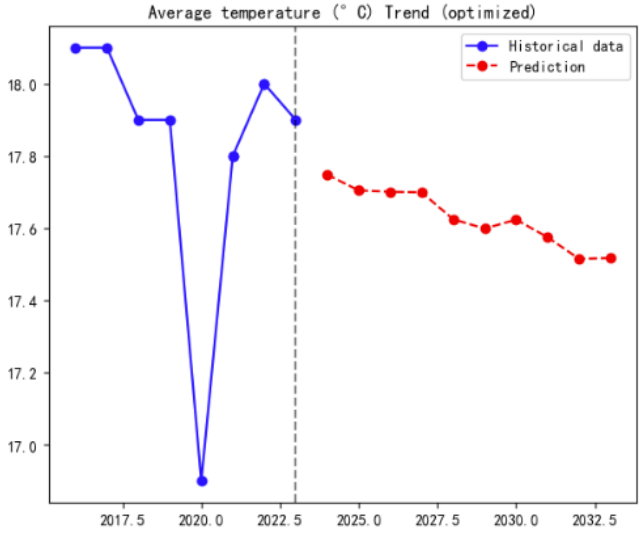

Figure 16. Projected temperature trends in Zhangjiajie, Hunan

By the same method, future climate trends in Zhangjiajie were predicted (Figure. 17). Results show rising average high temperatures but declining lows from 2024 onward. Actual 2024 data confirmed this: August highs reached 30°C (vs 2023's 28.3°C) and February lows dropped to 6°C (vs 6.7°C). Annual precipitation also matched predictions (2024: 1363.6mm vs 2023's 1018.6mm).

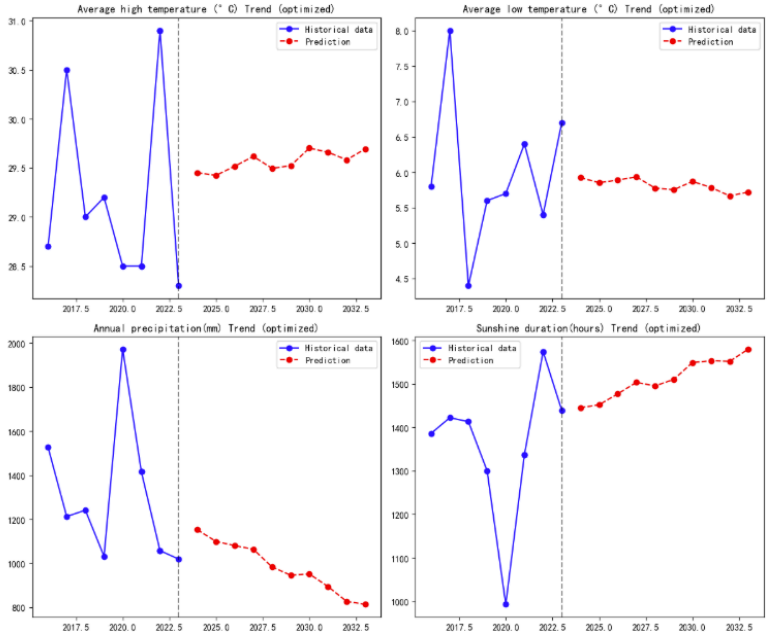

Figure 17. Projected climate trends: Zhangjiajie, Hunan

Climate change involves multiple factors. Short-term forecasts are accurate, but long-term predictions remain difficult. Despite global warming, La Niña still causes extreme temperature swings in China. Though limited by samples and computing power, this tree-based method complements existing research.

DOI: 10.54254/2753-8818/2026.34289

6. Conclusion and outlook

This study develops a laser diffraction method to quantify tree microstructural parameters and investigate their climate dependencies. Through numerical modeling and analysis of osmanthus/fir samples, we establish that fiber dimensions correlate positively with precipitation and sunlight exposure (sunlight being more influential), while growth rates increase with lower temperature extremes and higher average temperatures. The diffraction-based approach not only enables efficient microstructural characterization but also provides a novel climate proxy, with machine learning predictions partially validated by observational data, offering new insights for dendroclimatology and materials analysis.

This study establishes a cost-effective dendro-microstructural approach for climate research, though with sampling constraints: ① Single-site sampling in Zhangjiajie's complex terrain causes meteorological data mismatches, and ② limited specimens reduce statistical significance. Future work should expand multi-climate sampling for generalizability and incorporate fossilized/ancient wood to extend the timeline to centennial scales (requiring model adaptation). While currently focused on recent warming, the method shows promise for paleoclimate reconstruction.

References

[1] The Intergovernmental Panel on Climate Change, Sixth Assessment Report, Climate Change 2021: The Physical Science Basis [R], 2011, https: //www.ipcc.ch/assessment-report/ar6/.
[2] Alves E E N. Soil and tree X-ray spectroscopy analysis of Brazilian tropical mangrove ecosystem [D], Universidade Federal de Viçosa, 2018.
[3] Almeida T H, Sardela M, Lahr F A R. X-ray diffraction on aged Brazilian wood species [J]. Materials Science and Engineering: B, 2019, 246: 96-103.
[4] Borysiak S, Doczekalska B. X-ray diffraction study of pine wood treated with NaOH [J]. Fibres Text. East. Eur, 2005, 13(5): 87-89.
[5] Jang H F, Robertson A G, Seth R S. Transverse dimensions of wood pulp fibres by confocal laser scanning microscopy and image analysis [J]. Journal of materials science, 1992, 27(23): 6391-6400.
[6] Nowak J, Florek M, Kwiatek W, et al. Composite structure of wood cells in petrified wood [J]. Materials Science and Engineering: C, 2005, 25(2): 119-130.
[7] Begum S, Kudo K, Rahman M H, et al. Climate change and the regulation of wood formation in trees by temperature [J]. Trees, 2018, 32: 3-15.
[8] Pandey S. Climatic influence on tree wood anatomy: a review [J]. Journal of Wood Science, 2021, 67(1): 24.
[9] Olivar J, Rathgeber C, Bravo F. Climate change, tree-ring width and wood density of pines in Mediterranean environments [J]. Iawa Journal, 2015, 36(3): 257-269.
[10] Teodorescu I, Țăpuși D, Erbașu R, et al. Influence of the climatic changes on wood structures behaviour [J]. Energy Procedia, 2017, 112: 450-459.